*Desalination and Water Treatment*
www.deswater.com

doi: 10.5004/dwt.2018.22354

114 (2018) 332–340
May

# Preparation of eco-friendly activated carbon as a refining solution for the adsorptive treatment of analgesic acetaminophen

K.Y. Foo*

*River Engineering and Urban Drainage Research Centre (REDAC), Engineering Campus, Universiti Sains Malaysia, 14300 Nibong Tebal, Penang, Malaysia, Tel. +6045996539; Fax: +6045996926; email: k.y.foo@usm.my*

Received 20 January 2017; Accepted 8 April 2018

**ABSTRACT**

This study explores the feasibility of durian seed as an alternative precursor for the preparation of eco-friendly activated carbon (DSAC) via physiochemical activation. The porosity, functionality, and surface chemistry of DSAC were featured by means of low-temperature nitrogen adsorption–desorption curve, elemental analysis, scanning electron microscopy, Fourier transform infrared spectroscopy, evaluation of surface acidity/basicity, and zeta potential measurement. The adsorption behavior was examined by performing batch adsorption experiments using acetaminophen (ACT) as the model pollutant. Experimental data were simulated using the Freundlich, Langmuir, Temkin, and Dubinin–Radushkevich isotherm models. Kinetic modeling was fitted to the pseudo-first-order and pseudo-second-order equations. Results illustrated an encouraging performance toward the removal of ACT, with a monolayer adsorption capacity of 304.48 mg/g. The adsorption equilibrium was best confronted to the pseudo-second-order kinetic model, while the adsorptive removal of ACT onto DSAC was satisfactorily described by the Langmuir isotherm model. The findings demonstrated the applicability of DSAC as a promising adsorbent for the adsorptive treatment of analgesic ACT from the pharmaceutical contaminated wastewater.

*Keywords:* Acetaminophen; Activated carbon; Adsorption; Durian seed; Pharmaceutical

## 1. Introduction

The worldwide consumption of pharmaceuticals has increased significantly since 1950s as a direct result of the fast emerging medical science development [1]. In the last two decades, these pharmaceuticals and personal care products have raised scientific and public concerns regarding their low biodegradability, continuous pseudo-persistent properties, and potential contamination on the biological equilibrium of natural media and human health [2]. It is well established that these emerging pollutants and their metabolites, notably in the form of antibiotics, analgesics, psychotropics, antipyretics, and anti-inflammatories, constitute the important pathway of a wide array of toxic substances released into the environmental matrices [3].

According to Runnalls et al. [4], approximately 150 of pharmaceutical compounds, including a vast amount of antibiotics, anesthetics, disinfectants, heavy metals, adsorbable organic halogens, and cytostatic agents have been detected, in the surface water, groundwater table, and more recently drinking water. The continuous presence of these constituents, even at subtherapeutic concentrations, indicates an external exposure to the public health, flora, fauna and represents a sharp threat to the food chain ecosystems [5]. If poorly managed, it may become a hydrogeological contamination to synergize acute toxicity and genotoxicity, to retard photosynthetic activities in the aquatic life, inhibit the growth of biota, affect the symbiotic process, and damage the quality of the receiving streams [6]. Additionally, prolonged exposure to medical effluents could induce increased heart rate, vomiting, shock, Heinz body formation, cyanosis, jaundice, quadriplegia, tissue necrosis, allergy, dermatitis, eye or skin infections, irritation, and illustrate carcinogenic and mutagenic effects [7].

* Corresponding author.

Among all, acetaminophen (ACT), also known as paracetamol or 4-hydroxyacetanilide, stands out to be the most commonly applied analgesic and antipyretic compound for its effectiveness in the relief of fever, headaches, and other minor aches [8]. In combination with nonsteroidal anti-inflammatory drugs, ACT has been widely used in handling more severe pain, and appears to be the major ingredient in numerous cold and flu remedies [9]. However, it is characterized by the high solubility and mobility in the aquatic environment, and ubiquitously present in all sorts of streams and river waters from the concentration range of ng/L to mg/L [10]. This highlights the necessity of priority attention to identify a dedicated pretreatment method of pharmaceutical effluents.

Results from the previous studies have demonstrated the disadvantages of conventional treatment technologies for the effective treatment of pharmaceutical residues, with a low efficacy and formation of toxic by-products [11,12]. Activated carbons adsorption process, a separation process by which certain components of a fluid phase are attracted to the surface of carbon adsorbent, and form attachments via physical or chemical bonds [13], has been proposed to be a refining step for the remediation of pharmaceutical residues. The selection is due to its simplicity of design, ease of operation, insensitivity to toxic substances and high removal capability, even from the dilute concentrations [14]. Despite its prolific use in water purification, the wide scale implementation is deteriorated by the poor economic feasibility associated with its manufacture and regeneration costs [15].

In this sense, the utilization of nonvaluable by-products or residues as renewable precursors for the preparation of activated carbons would be an interesting strategy to lower the production costs, and enables the conversion of negative-value waste into useful, value-added products [16]. The present work was undertaken to examine the potential of durian seed (DS) as an efficient precursor for the preparation of low-cost activated carbon by physiochemical activation. The batch adsorption behavior of ACT was investigated as a prerequisite step on a large scale, for the remediation of contaminated pharmaceutical effluents. Structural, functional, and surface chemistry of the prepared adsorbent were evaluated. The effects of initial concentration, contact time, and solution pH on the adsorption performance were evaluated. Moreover, the adsorption isotherms, kinetics, thermodynamics, and regeneration study are outlined.

## 2. Materials and methods

### 2.1. Adsorbate

ACT, also known as paracetamol, with the molecular formula and molecular weight of $C_8H_9NO_2$ and 151.2 g/mole, respectively, was chosen as the targeted adsorbate in this study. A standard stock solution of 500 mg/L was prepared by dissolving an appropriate quantity of ACT in double distilled water. Working solutions of desired concentrations were prepared by successive dilution.

### 2.2. Preparation of activated carbon

DS used as raw material in this work was procured from a local plantation area. The raw precursors were manually chosen, washed exhaustively with distilled water to remove adhering impurities from the surface, air-dried, cut, and screened to the desired mesh size of 1–2 mm. The carbonization process was performed by loading 500 g of dried precursor into a vertical furnace, and heated up to a carbonization temperature of 500°C under purified $N_2$ flow (150 mL/min). The char produced was mixed in potassium hydroxide (KOH) solution with a char/KOH impregnation ratio of 1:1.5 (wt%) with occasional stirring.

The activated carbon was prepared by physiochemical activation method consisting of KOH treatment followed by carbon dioxide ($CO_2$) gasification. The activation process was carried out under the similar condition as carbonization, but to a final temperature of 800°C. Once the desired temperature was reached, the nitrogen gas flow was switched to $CO_2$, and held for 1 h. The activated product was cooled under inert atmosphere to the room temperature. The resultant activated carbon (DSAC) was washed with 0.1 M hydrochloric acid and rinsed repeatedly with hot and cold deionized water until pH 6–7 was reached in the washing solution.

### 2.3. Characterization of activated carbon

The surface morphology was imaged using the Zeiss Supra 35 VP scanning electron microscope equipped with W-Tungsten filament operated at 10–15 kV of speed voltage, 155 eV of resolution, and orientation of 35° with Mn $K_\alpha$ as the energy source. The pore structural analysis was characterized by nitrogen adsorption at 77 K with an accelerated surface area and porosimetry system (Micromeritics ASAP 2020). The specific surface area ($S_{BET}$) was calculated by the Brunauer–Emmett–Teller (BET) equation; the total pore volume ($V_T$) was evaluated by converting the adsorption volume of nitrogen at relative pressure of 0.95 to equivalent liquid volume of the adsorbate, while the micropore volume, micropore surface area, and external surface area were deduced using the *t*-plot method. Chemical characterization of surface functional groups was detected using the pressed potassium bromide (KBr) pellets containing 5% of carbon sample by Fourier transform infrared spectrometer (FTIR-2000, Perkin Elmer) in the scanning range of 4,000–400 $cm^{-1}$. The content of C, H, N, O, and S elements in the ultimate analysis was performed using an elemental analyzer.

### 2.4. Surface acidity and basicity

The surface acidity was estimated by mixing 0.20 g of DSAC with 25 $cm^3$ of 0.05 M NaOH solution in a closed flask, and agitated for 48 h at room temperature. The suspension was decanted, and the remaining NaOH was titrated with 0.05 M HCl. The surface basicity was measured by titration with 0.05 M NaOH after incubation of 0.20 g of DSAC with 0.05 M HCl.

### 2.5. Zeta potential measurement ($pH_{pzc}$)

The determination of $pH_{pzc}$ was conducted by adjusting the pH of 50 $cm^3$ of 0.01 M NaCl solution to a value between 2 and 12. 0.15 g of DSAC was added and the final pH was measured after 48 h under agitation. The $pH_{pzc}$ is the point where $pH_{initial} - pH_{final} = 0$.

*2.6. Batch equilibrium studies*

The batch adsorption experiments were undertaken in a set of 250 mL Erlenmeyer flasks containing 0.20 g of adsorbent and 200 mL of ACT solutions within the concentration range of 50–500 mg/L. The mixture was agitated at 30°C for a predetermined period using a thermostatic orbital shaker operated at an agitation speed of 120 rpm. The samples were collected at prescribed time intervals, and the analytical determination of ACT solution was performed spectrophotometrically using a double beam UV–Vis spectrophotometer (UV-1601 Shimadzu, Japan) at the maximum wavelength of 243 nm.

Each adsorption experiments were replicated at least three times and their arithmetical averages were used as the result. The adsorptive uptake of ACT at time $t$, $q_t$ (mg/g) and equilibrium, $q_e$ (mg/g), was calculated by:

$$q_t = \frac{(C_o - C_t)V}{W} \quad (1)$$

$$q_e = \frac{(C_o - C_e)V}{W} \quad (2)$$

where $C_o$, $C_t$, and $C_e$ (mg/L) are the liquid-phase concentrations of ACT at initial, time $t$ (min), and equilibrium, respectively. $V$ is the volume of the solution (L) and $W$ is the mass of adsorbent used (g). The effect of pH on ACT removal was examined by varying the pH from 2 to 12, with the initial ACT concentration of 500 mg/L, DSAC dosage of 0.20 g/200 mL, and adsorption temperature of 30°C. The initial pH of the ACT solution was adjusted by the addition of 0.10 M solution of HCl or NaOH.

## 3. Results and discussion

*3.1. Characterization of DSAC*

Nitrogen adsorption–desorption curve provides qualitative information on the adsorption mechanism and porous structure of the carbonaceous materials [17]. The isotherms of DSAC pertain to intermediate between type I and II of the referred International Union of Pure and Applied Chemistry (IUPAC) classification (Fig. 1(a)). This adsorption behavior exhibits a combination of microporous–mesoporous structure. The initial part of the isotherm represents micropore filling, and the slope of the plateau at high relative pressure is due to multilayer adsorption onto the external surface. Detailed characteristics of the porosity of DSAC are summarized in Table 1. It was inferred that the BET surface area, Langmuir surface area, and total pore volume of DSAC were identified to be 1,215.51 $m^2/g$, 1,809.10 $m^2/g$, and 0.687 $cm^3/g$, respectively.

Pore size distribution (PSD) is an important property that determines the fraction of the total pore volume accessible to molecules of a given size and shape [18]. According to the classification of IUPAC-pore dimensions, the pores of adsorbents are grouped into micropore ($d$ < 2 nm), mesopore ($d$ = 2–50 nm), and macropore ($d$ > 50 nm). The PSD of DSAC was ascertained using the density functional theory model by minimizing the grand potential as a function of fluid

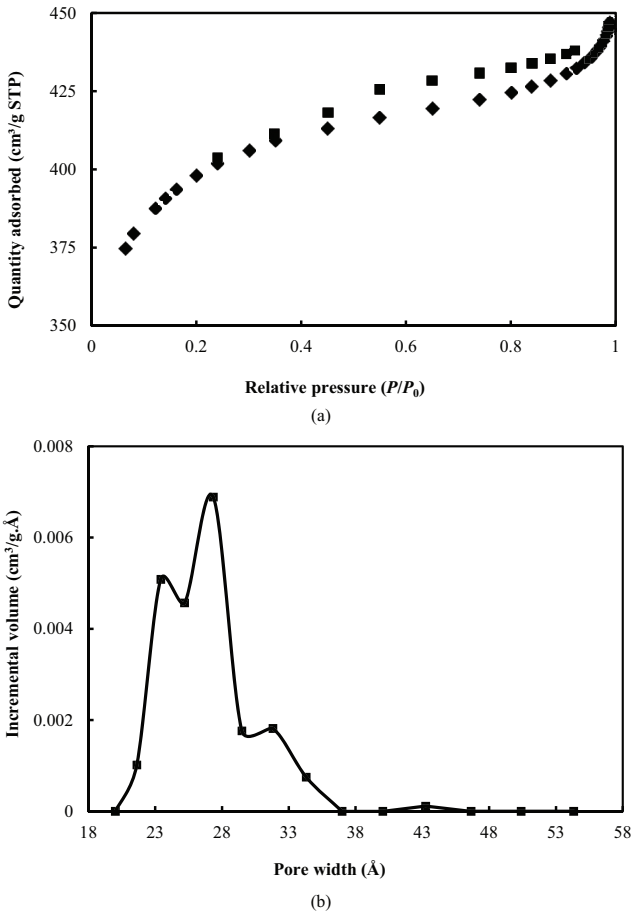


Fig. 1. Nitrogen adsorption–desorption curve (a) and pore size distribution (b) of DSAC according to the density functional theory (DFT) model.

Table 1
Porosity structures, chemical compositions, surface acidity and basicity of DSAC

| Properties | | DSAC |
|---|---|---|
| BET surface area ($m^2/g$) | | 1,215.51 |
| Micropore surface area ($m^2/g$) | | 646.34 |
| External surface area ($m^2/g$) | | 309.10 |
| Langmuir surface area ($m^2/g$) | | 1,809.10 |
| Total pore volume ($cm^3/g$) | | 0.687 |
| Micropore volume ($cm^3/g$) | | 0.207 |
| Mesopore volume ($cm^3/g$) | | 0.480 |
| Average pore size (nm) | | 2.261 |
| Acidity (mmole/g) | | 0.950 |
| Basicity (mmole/g) | | 1.225 |
| Total content of surface oxides (mmole/g) | | 2.175 |
| Element (%) | Carbon | 78.55 |
| | Oxygen | 17.07 |
| | Hydrogen | 4.25 |
| | Nitrogen | 0.11 |
| | Sulfur | 0.02 |

density profile, as depicted in Fig. 1(b). Result detected the sharpest peak at pore diameter between 2.0 and 4.0 nm, with an average pore size of 2.26 nm, showing a vast majority of the pores fall within the range of mesoporous structures.

The surface physical morphology of DSAC was examined using the scanning electron micrograph with a magnification of 500×, as depicted in Fig. 2. There were plenty of well pronounced, even, and developed pores over the surface of DSAC, forming an orderly pore structure. These cavities were resulted from the evaporation of impregnated KOH-derived compounds, leaving the space previously occupied by the reagent. The chemical compositions of DSAC is listed in Table 1. As suggested by the result, DSAC contains heteroatom mixture of carbon, hydrogen, oxygen, nitrogen, and sulfur. The carbon content of DSAC was 78.55%, while the content of oxygen, hydrogen, nitrogen, and sulfur was 17.07%, 4.25%, 0.11%, and 0.02%, respectively. This might be due to the pyrolytic effect at high temperature where most of the organic substances have been degraded and discharged both as gas and liquid tars leaving the high carbon purity [19].

The representative FTIR spectrum of DSAC is presented in Fig. 3. The region between 3,965 and 3,572 $cm^{-1}$ is attributed to the in-plane O–H (hydroxyl) groups. The transmittance at 3,234 $cm^{-1}$ is ascribed to the N–H groups. The presence of –C–H stretch of alkanes shows an intensity at 2,867 $cm^{-1}$, while the signal at 1,420 $cm^{-1}$ is identical to the vibration of $–CH_2$ (alkyl). Similarly, the sharp peaks at 1,053 and 828 $cm^{-1}$ are corresponded to the C–O (anhydrides) and out-of-plane N–O derivatives. The presence of these surface alkaline groups imparts a polar character to the DSAC surface, which can affect the preferential adsorption of polar acidic pharmaceutical pollutants such as ACT.

The surface acidity and basicity are important criterion interpreting the surface chemistry of the carbon adsorbents [20]. Analysis of the data from Table 1 shows that DSAC exhibited an alkaline character, with the surface acidity of 0.95and 1.23 mmole/g of surface basicity. The surface basicity is related to the presence of oxygen-free Lewis sites and carbonyls, pyrone and chromene type structures, while the carbon acidity was derived primarily from the oxygen-containing groups (mainly carboxylic, anhydrides, lactones, and phenols) at the edge of the carbon layers. The zero point of charge ($pH_{ZPC}$), an index of the propensity of the surface charge as a function of pH, was measured using the acid/base titration method, and the $pH_{ZPC}$ of DSAC was 7.76.

### 3.2. Batch adsorption studies

Fig. 4(a) presents the variation of adsorption with respect to time at the concentrations of 50–500 mg/L. The adsorptive removal of ACT increased with prolonging the contact time. It is clear from Fig. 4(a) that the adsorption process increased sharply at the initial stage, indicating the availability of readily accessible sites. The process was gradually slow down as the equilibrium approached. At this point, the amount of ACT desorbing from the adsorbent is in a state of dynamic equilibrium with the amount of ACT being adsorbed onto the activated carbon. The time required to attain this state of equilibrium is termed as equilibrium time. The amount of pollutants adsorbed at the equilibrium time reflects the maximum adsorption capacity of the adsorbent under those operating conditions [21].

Initial concentration provides an essential driving force for alleviating the mass transfer resistance between the aqueous phase and the solid medium [22]. In the present study, the adsorption equilibrium, $q_e$ increased from 51.93 to 306.60 mg/g with an increase in initial concentration from 50 to 500 mg/L. Conversely, there was a reverse relationship between the equilibrium concentrations with the initial ACT concentrations. The equilibrium concentration, $C_e$ obtained at 50, 100, 150, 200, 300, 400, and 500 mg/L was 0.19, 0.47, 1.82, 16.98, 101.77, and 200.32 mg/L, respectively, indicating high percentage removal of ACT even at high initial concentrations.

Besides, it can be deduced from the results that longer contact time was required for the ACT solution of higher concentrations to reach the equilibrium. The contact time needed for the ACT solution with initial concentration of 50–100 mg/L to reach the equilibrium was around 6 h, and for ACT solution of higher concentrations, 10–16 h was

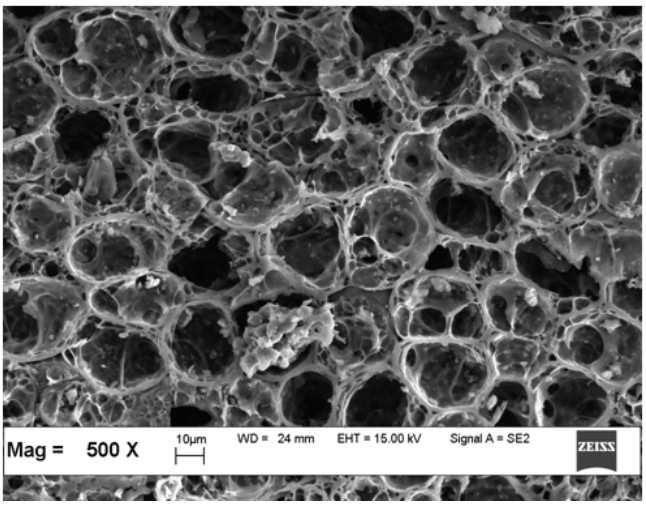


Fig. 2. Scanning electron micrograph of DSAC.

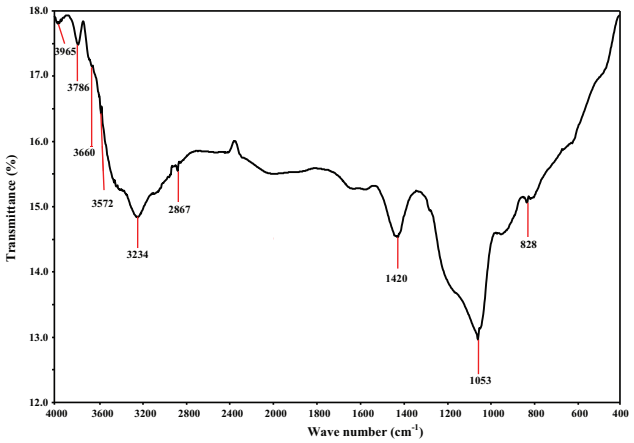


Fig. 3. FTIR spectrum of DSAC.

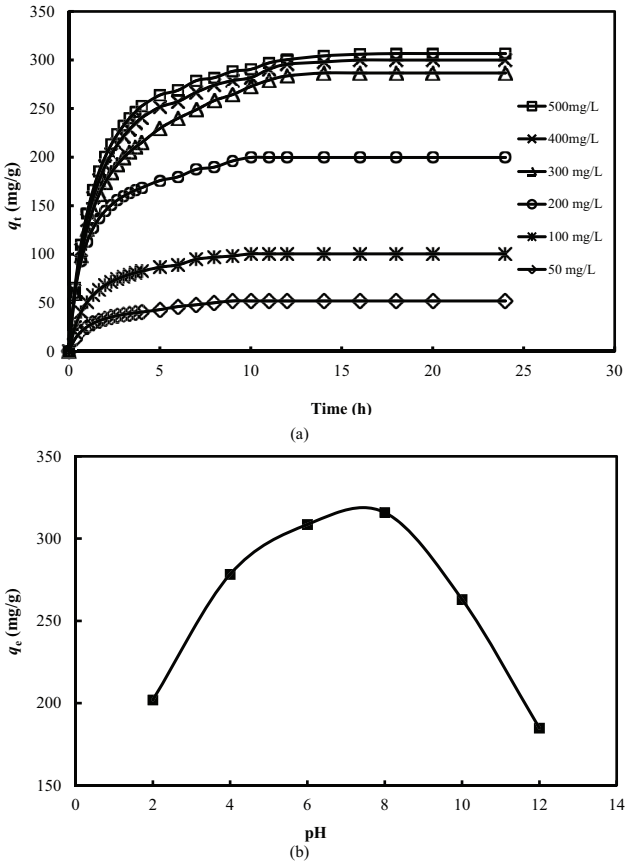


Fig. 4. The variation of adsorption with respect to time and initial ACT concentrations (a) and solution pH (b).

required. The observation could be explained by the fact that during the adsorption process, the ACT molecules had to first encounter the boundary layer, before they could diffuse into the adsorbent and adsorbed onto the binding surface. The time profile of ACT uptake is a single, smooth, and continuous curve leading to saturation, suggesting possible monolayer coverage of ACT onto the surface of DSAC.

Solution pH exerts a profound influence on the adsorptive uptake of adsorbate molecule by regulating the surface charge and ionization/dissociation of the adsorbate molecules [23]. The adsorption behavior of ACT as a function of solution pH is depicted in Fig. 4(b). Increasing solution pH serves to increase the adsorption capacity, with a significant enhancement as the pH increased from pH 2 to 8. As ACT is a weak electrolyte, the carbon surface and the adsorbate species may coexist in a complex system, in which the same or opposite charges may be present, resulting in different adsorption interactions [24]. Lower adsorption at strong acidic pH of 2–4 is due to the protonation of ACT, and high mobility of $H_3O^+$ ions competing with ACT cations for the adsorption sites.

In the strong basic medium of 10–12, it is postulated that the reduction of the adsorption uptake of ACT is mainly ascribed to the repulsion effect between the $OH^-$ ions with the carbon basic surface sites. Hoegberg et al. [25] suggested that ACT maintains its nonionized form (which is less sensitive to pH), and is adsorbed onto activated charcoal at pH values <9.38. However, it could be converted to a negative charge from the protonated base in basic solutions (pH >9.38). Following this mechanism, the adsorption of ACT onto DSAC showed the greatest performance at the pH range of 6–8.

### 3.3. Adsorption kinetics

Adsorption kinetics describes the solute uptake rate (chemical reaction), which in turn governs residence time of the adsorption process [26]. When adsorption is preceded by diffusion through a boundary, the kinetics in most systems follow the pseudo-first-order rate equation. Lagergren [27] proposed pseudo-first-order kinetic equation in the form of:

$$\ln\left(\frac{q_e}{q_e - q_t}\right) = \frac{k_1}{2.303}t \tag{3}$$

Contrary to pseudo-first-order equation, pseudo-second-order equation [28] predicts the behavior over the whole range of adsorption represented by:

$$\frac{1}{\left(q_e - q_t\right)} = \frac{1}{q_e} + k_2 t \tag{4}$$

To better comprehend and analyze the adsorption process, the experimental data at different time intervals were simulated by the pseudo-first-order and pseudo-second-order kinetic models, using the plots $\ln(q_e - q_t)$ against $t$, and $t/q_t$ versus $t$, respectively. The applicability of the kinetic equation was judged by the determination of the coefficient of determination, $R^2$.

$$R^2 = \frac{\sum(q_{\text{cal}} - q_{m,\text{exp}})^2}{\sum(q_{\text{cal}} - q_{m,\text{exp}})^2 + (q_{\text{cal}} - q_{m,\text{exp}})^2} \tag{5}$$

where $q_{\text{exp}}$ (mg/g) and $q_{\text{cal}}$ (mg/g) are the experimental and calculated adsorption capacity, respectively, while $q_{m,\text{exp}}$ is the average $q_{\text{exp}}$ (mg/g). The suitability of the kinetic model to describe the adsorption process was further validated by the normalized standard deviation, $\Delta q$ (%) given by:

$$\Delta q = 100\sqrt{\frac{\Sigma[(q_{\text{exp}} - q_{\text{cal}})/q_{\text{exp}}]^2}{n-1}} \tag{6}$$

where $n$ is the number of data points. The corresponding results are tabulated in Table 2. Pseudo-second-order kinetic model led to good fittings of the experimental results, with the correlation coefficient values, $R^2$ greater than 0.99, and the lowest normalized standard deviation, $\Delta q$ values, which ranged between 1.88% and 11.23% for all the tested concentrations. This suggested that the adsorption system follows the pseudo-second-order model, based on the assumption that the rate-limiting step may be chemisorption, which involves valence forces through electrons sharing between the hydrophilic edges sites of DSAC and ACT cations.

Table 2
Kinetic models parameters for the adsorption of ACT onto DSAC at different initial ACT concentrations

| $C_o$ (mg/L) | $q_{e,exp}$ (mg/g) | Pseudo-first-order | | | | Pseudo-second-order | | | |
|---|---|---|---|---|---|---|---|---|---|
| | | $k_1$ ($h^{-1}$) | $q_{e,cal}$ (mg/g) | $R^2$ | $\Delta q$ (%) | $k_2$ (×$10^3$) (g/mg h) | $q_{e,cal}$ (mg/g) | $R^2$ | $\Delta q$ (%) |
| 50 | 51.93 | 0.395 | 39.96 | 0.953 | 23.05 | 19.756 | 51.93 | 0.998 | 2.59 |
| 100 | 100.41 | 0.411 | 79.35 | 0.960 | 20.97 | 8.945 | 100.41 | 0.999 | 4.15 |
| 200 | 199.63 | 0.422 | 151.47 | 0.946 | 24.13 | 5.929 | 199.63 | 1.000 | 1.60 |
| 300 | 286.58 | 0.373 | 257.57 | 0.971 | 10.12 | 2.880 | 286.58 | 0.999 | 1.88 |
| 400 | 299.91 | 0.306 | 323.18 | 0.966 | 7.76 | 2.190 | 299.91 | 0.989 | 8.34 |
| 500 | 306.59 | 0.307 | 339.00 | 0.962 | 10.57 | 2.090 | 306.60 | 0.989 | 11.23 |

### 3.4. Adsorption thermodynamic

Thermodynamic is a critical aspect predicting the stability of the solid–liquid phase equilibrium. Its original concepts assume that energy cannot be gained or lost, which entropy change is the driving force in an isolated system [29]. In this work, the values of enthalpy change ($\Delta H$), Gibbs free energy change ($\Delta G$), and entropy change ($\Delta S$) at the adsorption temperature of 30°C, 40°C, and 50°C were computed by the equations:

$$\ln K_L = \frac{\Delta S}{R} - \frac{\Delta H}{RT} \tag{7}$$

$$\Delta G = -RT \ln K_L \tag{8}$$

where $R$ (8.314 J/mole K) is the universal gas constant, $T$ (K) is the absolute solution temperature, and $K_L$ (L/mg) is the Langmuir isotherm constant. The values of $\Delta H$ and $\Delta S$ were determined from the slope and intercept of the van't Hoff plot of ln $K_L$ versus $1/T$ [30]. The calculated thermodynamic parameters are listed in Table 3. The positive value of $\Delta S$ revealed the affinity of DSAC for the adsorbate being tested, and increasing randomness at the solid–solution interface during the fixation of ACT onto the active sites of DSAC.

The positive values of $\Delta H$ represented endothermic of the adsorption interaction. The result implied that the adsorption of ACT onto DSAC was highly temperature dependent. This endothermic process was attributed to the acceleration of diffusion rate of the ACT species across the external boundary layer, and in the internal pores of DSAC. Another possible explanation could be attending to the relation between the dimension of ACT species that can be present in solution, and at the mesoporous–microporous network of the adsorbent surface. The critical dimensions of ACT monomers are close to the opening of the pores correspondent to the maximum of the micropore size distribution of the carbon sample. As the temperature increased from 30°C to 50°C, the vibration energy of the molecules would increase, favoring the accessibility of the species to the microporosity with widths near to the critical dimensions of the molecule, which in turn increased the adsorptive uptake [31].

Negative $\Delta G$ dictated spontaneous nature and feasibility of the adsorption process with high preference of ACT onto the prepared activated carbon. The value of $\Delta G$ was −0.133 kJ/mole at 30°C, and this $\Delta G$ value turned lower at the higher operating temperatures of 40°C and 50°C. This showed that the reaction rate increased with increasing the operating temperature. The results were consistent with the earlier findings [32,33], where the adsorption of ACT onto DSAC was endothermic in nature.

Table 3
Thermodynamic parameters for the adsorption of ACT onto DSAC

| $\Delta H°$ (kJ/mole) | $\Delta S°$ (J/mole K) | $\Delta G°$ (kJ/mole) | | |
|---|---|---|---|---|
| | | 303 K | 313 K | 323 K |
| 11.99 | 39.98 | –0.133 | –0.485 | –0.935 |

### 3.5. Adsorption isotherm

Adsorption isotherm is viable to reveal the specific affinity and sorption mechanism of the carbonaceous adsorbents. The correlation is important for practical design and fundamental understanding of the adsorption systems [34]. Due to the inherent bias resulting from linearization, alternative isotherm parameter sets were determined by nonlinear regression. In this study, the nonlinear Freundlich [35], Langmuir [36], Temkin [37], and Dubinin–Radushkevich [38] isotherm models were established:

$$q_e = K_F C_e^{1/n} \tag{9}$$

$$q_e = \frac{Q_0 K_L C_e}{1 + K_L C_e} \tag{10}$$

$$q_e = B \ln\left(AC_e\right) \tag{11}$$

$$q_e = q_s \exp(-k_{ad}\varepsilon^2) \tag{12}$$

where $Q_0$ (mg/g) is the Langmuir isotherm constant related to adsorption capacity, and $K_F$ (mg/g) (L/mg) and $1/n$ are the Freundlich isotherm constant, and a measure of the adsorption intensity. $B = RT/b$, where $b$ and $A$ are the Temkin isotherm constant related to heat of sorption (J/mole) and equilibrium binding constant (L/g). $q_s$ (mg/g) is denoted as the theoretical isotherm saturation capacity, and $\varepsilon$ can be correlated as:

$$\varepsilon = RT \ln\left[1 + \frac{1}{C_e}\right] \tag{13}$$

The constant $B_{DR}$ gives the mean free energy, $E$ (J/mole) of sorption per molecule of the adsorbate when it is transferred to the surface of solid from infinity in the solution, and can be determined by the relationship:

$$E = \left[\frac{1}{\sqrt{2B_{DR}}}\right] \tag{14}$$

For nonlinear regression, a trial and error procedure, which is applicable to computer operation, was developed to determine the isotherm parameters by maximizing the respective coefficient of determination between experimental data and the isotherms. The applicability of the isotherm models was judged by determining the correlation coefficients, $R^2$, where the higher the $R^2$ value, the better the fit is. The validity of the models was further verified by root-mean-square deviation (RMSD), the commonly used statistical tool measuring the predictive power of a model derived as:

$$\text{RMSD} = \frac{\sqrt{\sum_{i=1}^{n}(q_{\text{exp}} - q_P)^2}}{n-1} \tag{15}$$

where $q_{\text{exp}}$ (mg/g) and $q_P$ (mg/g) are the experimental and theoretical adsorption capacities, respectively.

The statistical correlations reported in Table 4 showed strong positive evidence that the adsorption of ACT onto DSAC followed Langmuir isotherm model, with the lowest RMSD and $R^2$ values higher than 0.99, as compared with the other models. The applicability of Langmuir isotherm model suggested that the adsorption takes place on homogeneous sites within the adsorption site; with each molecule possess constant enthalpies and sorption activation energy. The results also demonstrated no interaction and transmigration of ACT in the plane of the neighboring surface. Table 5 summarizes a comparative evaluation of the monolayer adsorption capacities for ACT onto various adsorbents [31,39–45]. It can be concluded that the activated carbon prepared in this work showed relatively high adsorption capacity of 304.48 mg/g, as compared with the previous researches.

### 3.6. Regeneration study

The regeneration study was conducted by rinsing the ACT-loaded DSAC with ethanol solution, subsequently by extensive washing with deionized water. The regenerated samples were air dried at 120°C, and applied for the next adsorption–regeneration cycles. The result is presented in Fig. 5. It was evident that there was no appreciable difference between the adsorptive uptake of PCM onto the regenerated samples as compared with the virgin DSAC, even after several adsorption–regeneration cycles. The slight decrease in the adsorptive uptake of ACT at the subsequent regeneration cycle might be due to the pore blockage as a consequence of incomplete desorption of adsorbate molecules retained in the carbon network, and the loss of DSAC during the adsorption–regeneration process, resulting in lower active sites for the adsorption of ACT molecules. The findings highlighted the stability of DSAC, to maintain its high adsorptive uptake at 280.58–272.66 mg/g even after five regeneration runs. The successive results from the regeneration study demonstrated the high economic feasibility of DSAC to be applied for different environmental decontamination process.

Table 5
A comparative evaluation of the monolayer adsorption capacities for ACT onto various adsorbents

| Adsorbent | Monolayer adsorption capacity (mg/g) | Reference |
|---|---|---|
| DSAC | 304.48 | Present study |
| Fly ash-activated carbon mixture | 232.60 | [31] |
| Commercial activated carbon | 286.40 | [39] |
| Montmorillonite/*N*-(carboxyacyl) chitosan nanocomposite | 33.73 | [40] |
| Xerogel | 3.11 | [41] |
| Modified grape stalk | 2.18 | [42] |
| Graphene nanoplatelets | 18.07 | [43] |
| Cork powder activated carbon | 200.00 | [44] |
| Peach stone activated carbon | 204.00 | [44] |
| Biochar | 28.43 | [45] |

Table 4
Isotherm parameters for the adsorption of ACT onto DSAC

| Isotherms | Constants | | | |
|---|---|---|---|---|
| Freundlich | $n$ | $K_F$ (mg/g).(L/mg)$^{1/n}$ | $R^2$ | RMSD |
| | 6.21 | 143.38 | 0.829 | 16.92 |
| Langmuir | $Q_0$ (mg/g) | $K_L$ (L/mg) | $R^2$ | RMSD |
| | 304.48 | 1.05 | 0.999 | 0.776 |
| Temkin | $A$ (L/g) | $B$ | $R^2$ | RMSD |
| | 46.93 | 36.61 | 0.918 | 11.73 |
| Dubinin–Radushkevich | $q_s$ (mg/g) | $E$ (J/mole) | $R^2$ | RMSD |
| | 285.68 | 1,994.42 | 0.937 | 10.276 |

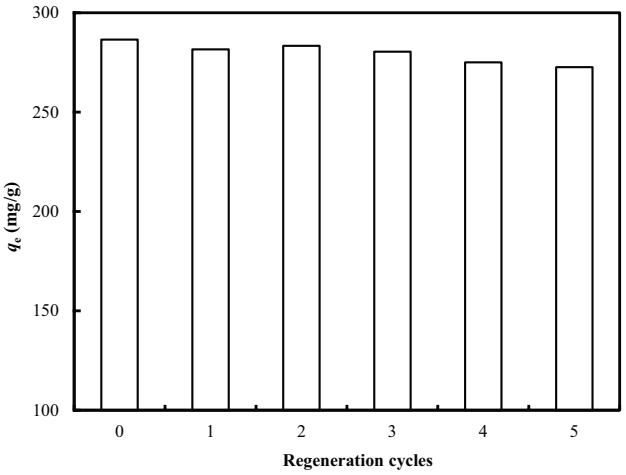


Fig. 5. The variation of adsorption uptake of ACT in the five adsorption-regeneration cycles.

## 4. Conclusion

This study revealed the potential of DS as a suitable candidate for the manufacture of activated carbon with a well-developed porous texture. This has attempted a new path for multipurpose utilization of the durian solid residue. The prepared activated carbon attained the maximum BET surface area of 1,215.51 $m^2/g$, total pore volume of 0.687 $cm^3/g$, and a high contribution of mesopores of 70%. Adsorption equilibrium was satisfactorily represented by the Langmuir isotherm, with a monolayer adsorption capacity of 304.48 mg/g. The kinetic data agreed satisfactorily with the pseudo-second-order kinetic model, suggesting a chemisorption process. Positive $\Delta H°$ value indicated the endothermic nature of the adsorptive interaction, while negative $\Delta G°$ verified the feasibility of the adsorption process.

## Acknowledgments

The author acknowledges the financial support provided by Universiti Sains Malaysia under the Research University (RUI) (Project no. 1001/PREDAC/814272) and USM Bridging (Project no. 304/PREDAC/6316095) grant schemes.

## References

[1] K.S. Le Corre, C. Ort, D. Kateley, B. Allen, B.I. Escher, J. Keller, Consumption-based approach for assessing the contribution of hospitals towards the load of pharmaceutical residues in municipal wastewater, Environ. Int., 45 (2012) 99–111.
[2] J. Akhtar, N.A.S Amin, K. Shahzad, A review on removal of pharmaceuticals from water by adsorption, Desal. Wat. Treat., 57 (2016) 12842–12860.
[3] L. Bo, N. Gao, J. Liu, B. Gao, The competitive adsorption of pharmaceuticals on granular activated carbon in secondary effluent, Desal. Wat. Treat., 57 (2016) 17023–17029.
[4] T.J. Runnalls, L. Margiotta-Casaluci, S. Kugathas, J.P. Sumpter, Pharmaceuticals in the aquatic environment: steroids and anti-steroids as high priorities for research, Hum. Ecol. Risk Assess., 16 (2010) 1318–1338.
[5] J. Hu, R. Shang, M. Frolova, B. Heijman, L. Rietveld, Pharmaceutical adsorption from the primary and secondary effluents of a wastewater treatment plant by powdered activated carbon, Desal. Wat. Treat., 57 (2016) 21304–21313.
[6] A. Mendoza, J. Aceña, S. Pérez, M.L. de Alda, D. Barceló, A. Gil, Y. Valcárcel, Pharmaceuticals and iodinated contrast media in a hospital wastewater: a case study to analyse their presence and characterise their environmental risk and hazard, Environ. Res., 140 (2015) 225–241.
[7] S. Harris, C. Morris, D. Morris, M. Cormican, E. Cummins, Antimicrobial resistant *Escherichia coli* in the municipal wastewater system: effect of hospital effluent and environmental fate, Sci. Total Environ., 468 (2014) 1078–1085.
[8] A. Mashayekh-Salehi, G. Moussavi, Removal of acetaminophen from the contaminated water using adsorption onto carbon activated with $NH_4Cl$, Desal. Wat. Treat., 57 (2016) 12861–12873.
[9] S. Cheng, J. Wu, H. Xia, J. Peng, S. Wang, L. Zhang, Microwave-assisted regeneration of spent activated carbon from paracetamol wastewater plant using response surface methodology, Desal. Wat. Treat., 57 (2016) 18981–18991.
[10] L. Feng, E.D. van Hullebusch, M.A. Rodrigo, G. Esposito, M.A Oturan, Removal of residual anti-inflammatory and analgesic pharmaceuticals from aqueous systems by electrochemical advanced oxidation processes. A review, Chem. Eng. J., 228 (2013) 944–964.
[11] C. Gadipelly, A. Pérez-González, G.D. Yadav, I. Ortiz, R. Ibáñez, V.K. Rathod, K.V. Marathe, Pharmaceutical industry wastewater: review of the technologies for water treatment and reuse, Ind. Eng. Chem. Res., 53 (2014) 11571–11592.
[12] Y. Li, R. Jindal, K. Choi, Y.L. Kho, P.G. de Bullen, Pharmaceutical residues in wastewater treatment plants and surface waters in Bangkok, J. Hazard. Toxic Radioact. Waste, 16 (2011) 88–91.
[13] K.Y. Foo, L.K. Lee, B.H. Hameed, Preparation of tamarind fruit seed activated carbon by microwave heating for the adsorptive treatment of landfill leachate: a laboratory column evaluation, Bioresour. Technol., 133 (2013) 599–605.
[14] K.Y. Foo, B.H. Hameed, A rapid regeneration of methylene blue dye-loaded activated carbons with microwave heating, J. Anal. Appl. Pyrolysis, 98 (2012) 123–128.
[15] K.Y. Foo, B.H. Hameed, A cost effective method for regeneration of durian shell and jackfruit peel activated carbons by microwave irradiation, Chem. Eng. J., 193 (2012) 404–409.
[16] K.Y. Foo, B.H. Hameed, Dynamic adsorption behavior of methylene blue onto oil palm shell granular activated carbon prepared by microwave heating, Chem. Eng. J., 203 (2012) 81–87.
[17] K.Y. Foo, L.K. Lee, B.H. Hameed, Preparation of banana frond activated carbon by microwave induced activation for the removal of boron and total iron from landfill leachate, Chem. Eng. J., 223 (2013) 604–610.
[18] K.Y. Foo, Value-added utilization of maize cobs waste as an environmental friendly solution for the innovative treatment of carbofuran, Process Saf. Environ. Prot., 100 (2016) 295–304.
[19] K.Y. Foo, B.H. Hameed, Preparation and characterization of activated carbon from melon (*Citrullus vulgaris*) seed hull by microwave-induced NaOH activation, Desal. Wat. Treat., 47 (2012) 130–138.
[20] K.Y. Foo, Effect of microwave regeneration on the textural network, surface chemistry and adsorptive property of the agricultural waste based activated carbons, Process Saf. Environ. Prot., 116 (2018) 461–467.
[21] K.Y. Foo, L.K. Lee, B.H. Hameed, Preparation of activated carbon from sugarcane bagasse by microwave assisted activation for the remediation of semi-aerobic landfill leachate, Bioresour. Technol., 134 (2013) 166–172.
[22] S.F.A. Shattar, N.A. Zakaria, K.Y. Foo, Utilization of montmorillonite as a refining solution for the treatment of ametryn, a second generation of pesticide, J. Environ. Chem. Eng., 5 (2017) 3235–3242.
[23] K.Y. Foo, L.K. Lee, B.H. Hameed, Batch adsorption of semi-aerobic landfill leachate by granular activated carbon prepared by microwave heating, Chem. Eng. J., 222 (2013) 259–264.
[24] B. Ruiz, I. Cabrita, A.S. Mestre, J.B. Parra, J. Pires, A.P. Carvalho, C.O. Ania, Surface heterogeneity effects of activated carbons on the kinetics of paracetamol removal from aqueous solution, Appl. Surf. Sci., 256 (2010) 5171–5175.

[25] L.C.G. Hoegberg, H.R. Angelo, A.B. Christophersen, H.R. Christensen, Effect of ethanol and pH on the adsorption of acetaminophen (paracetamol) to high surface activated charcoal, in vitro studies, J. Toxicol. Clin. Toxicol., 40 (2002) 59–67.
[26] S.F.A. Shattar, N.A. Zakaria, K.Y. Foo, Enhancement of hazardous pesticide uptake, ametryn using an environmentally friendly clay-based adsorbent, Desal. Wat. Treat., 79 (2017) 188–195.
[27] S. Lagergren, Zur theorie der sogenannten adsorption geloester stoffe, Veternskapsakad Handlingar, 24 (1898) 1–39.
[28] Y.S. Ho, Adsorption of Heavy Metals from Waste Streams by Peat, Ph.D. Thesis, University of Birmingham, Birmingham, UK, 1995.
[29] E.A. Khan, T.A. Khan, Adsorption of methyl red on activated carbon derived from custard apple (*Annona squamosa*) fruit shell: equilibrium isotherm and kinetic studies, J. Mol. Liq., 249 (2018) 1195–1211.
[30] J.H. van't Hoff, Die Rolle osmotischen Drucks in der Analogie zwischen Losungen und Gasen, Z. Phys. Chem., 1 (1887) 481–508.
[31] M. Galhetas, A.S. Mestre, M.L. Pinto, I. Gulyurtlu, H. Lopes, A.P. Carvalho, Carbon-based materials prepared from pine gasification residues for acetaminophen adsorption, Chem. Eng. J., 240 (2014) 344–351.
[32] G.Z. Kyzas, N.K. Lazaridis, C.A. Mitropoulos, Removal of dyes from aqueous solutions with untreated coffee residues as potential low-cost adsorbents: equilibrium, reuse and thermodynamic approach, Chem. Eng. J., 189 (2012) 148–159.
[33] J.X. Lin, S.L. Zhan, M.H. Fang, X.Q. Qian, H. Yang, Adsorption of basic dye from aqueous solution onto fly ash, J. Environ. Manage., 87 (2008) 193–200.
[34] K.Y. Foo, B.H. Hameed, Insights into the modeling of adsorption isotherm systems, Chem. Eng. J., 156 (2010) 2–10.
[35] H. Freundlich, Über die adsorption in lösungen (adsorption in solution), Z. Phys. Chem., 57 (1906) 384–470.
[36] I. Langmuir, The adsorption of gases on plane surfaces of glass, mica and platinum, J. Am. Chem., 57 (1918) 1361–1403.
[37] M.I. Tempkin, V. Pyzhev, Kinetics of ammonia synthesis on promoted iron catalyst, Acta Phys. Chim. USSR, 12 (1940) 327–356.
[38] M.M. Dubinin, L.V. Radushkevich, The equation of the characteristic curve of the activated charcoal, Proc. Acad. Sci. USSR Phys. Chem. Sec., 55 (1947) 331–337.
[39] D.H. Valdes, C.E. Victorero, L.P. Lou, D.T. Perez, L.D. Pages, M. Arias, U.J. Haza, Interaction of paracetamol and $^{125}$I-paracetamol with surface groups of activated carbon: theoretical and experimental study, J. Radioanal. Nucl. Chem., 305 (2015) 609–622.
[40] T.S. Anirudhan, S.S. Gopal, S. Sandeep, Synthesis and characterization of montmorillonite/N-(carboxyacyl) chitosan coated magnetic particle nanocomposites for controlled delivery of paracetamol, Appl. Clay Sci., 88 (2014) 151–158.
[41] E.C. Morais, G.G. Correa, R. Brambilla, J.H.Z. dos Santos, A.G. Fisch, Selective silica-based sorbent materials synthesized by molecular imprinting for adsorption of pharmaceuticals in aqueous matrices, J. Sep. Sci., 36 (2013) 636–643.
[42] I. Villaescusa, N. Fiol, J. Poch, A. Bianchi, C. Bazzicalupi, Mechanism of paracetamol removal by vegetable wastes: the contribution of π–π interactions, hydrogen bonding and hydrophobic effect, Desalination, 270 (2011) 135–142.
[43] L.A. Al-Khateeb, S. Almotiry, M.A. Salam, Adsorption of pharmaceutical pollutants onto graphene nanoplatelets, Chem. Eng. J., 248 (2014) 191–199.
[44] I. Cabrita, B. Ruiz, A.S. Mestre, I.M. Fonseca, A.P. Carvalho, C.O. Ania, Removal of an analgesic using activated carbons prepared from urban and industrial residues, Chem. Eng. J., 163 (2010) 249–255.
[45] C. Jung, J. Oh, Y. Yoon, Removal of acetaminophen and naproxen by combined coagulation and adsorption using biochar: influence of combined sewer overflow components, Environ. Sci. Pollut. Res., 22 (2015) 10058–10069.